Published in final edited form as:
Exp Neurol. 2012 May ; 235(1): 188–196. doi:10.1016/j.expneurol.2011.11.015.

Comprehensive Locomotor Outcomes Correlate to Hyperacute Diffusion Tensor Measures After Spinal Cord Injury in the Adult Rat

Joong Kim[1], **Sheng-Kwei Song**[1], **Darlene A. Burke**[2], and **David S. K. Magnuson**[2]
[1]Department of Radiology, Washington University, St. Louis. MO 63110
[2]Department of Neurological Surgery, University of Louisville, Louisville. KY 40292

Abstract

In adult rats, locomotor deficits following a contusive thoracic spinal cord injury (SCI) are caused primarily by white matter loss/dysfunction at the epicenter. This loss/dysfunction decreases descending input from the brain and cervical spinal cord, and decreases ascending signals in long propriospinal, spinocerebellar and somatosensory pathways, among many others. Predicting the long-term functional consequences of a contusive injury acutely, without knowledge of the injury severity is difficult due to the temporary flaccid paralysis and loss of reflexes that accompanies spinal shock. It is now well known that recovery of high quality hindlimb stepping requires only 12-15% spared white matter at the epicenter, but that forelimb-hindlimb coordination and precision stepping (grid or horizontal ladder) requires substantially more trans-contusion communication. In order to translate our understanding of the neural substrates for functional recovery in the rat to the clinical arena, common outcome measures and imaging modalities are required. In the current study we furthered the exploration of one of these approaches, diffusion tensor magnetic resonance imaging (DTI), a technique now used commonly to image the brain in clinical research but rarely used diagnostically or prognostically for spinal cord injury. In the adult rat model of SCI, we found that hyper-acute (<3 hours post-injury) DTI of the lateral and ventral white matter at the injury epicenter was predictive of both electrophysiological and behavioral (locomotor) recovery at 4 weeks post-injury, despite the presence of flaccid paralysis/spinal shock. Regions of white matter with a minimum axial diffusivity of 1.5μm^2/ms at 3 hours were able to conduct action potentials at 4 weeks, and axial diffusivity within the lateral funiculus was highly predictive of locomotor function at 4 weeks. These observations suggest that acute DTI should be useful to provide functional predictions for spared white matter following contusive spinal cord injuries clinically.

Introduction

The adult rat T9 contusion model of spinal cord injury has been in use for more than two decades (Kwo et al., 1989) and, in combination with other injury models, has allowed us to build a strong understanding of the relationship between spared tissue and recovered functions (Schucht et al., 2002; Basso et al., 1996). Simplistically, hindlimb functional

Correspondence: David S. K. Magnuson, PhD Kentucky Spinal Cord Injury Research Center University of Louisville, Louisville, KY 40292 dsmagn01@louisville.edu (502)852-6551.

deficits and recovery in this model can be divided into locomotor (overground stepping or swimming) and sensorimotor (precision stepping)(Gale et al., 1985; Magnuson et al., 2009; Kuerzi et al., 2010). Contusion injuries that induce a complete loss of the dorsal columns and substantial reductions in lateral and ventral white matter can still result in significant recovery of open field stepping, without hindlimb/forelimb coordination, if as little as 12-15% of the total white matter is retained (Schucht et al, 2002; Basso et al., 1996; Kuerzi et al., 2010). Open field stepping that includes hindlimb/forelimb coordination appears to require 15-25% sparing of the total ventral white matter, but does not depend on the presence of dorsal column or corticospinal axons (Schucht et al., 2002; Basso et al., 1996; Loy et al., 2002a; 2002b). In contrast, precision stepping on a horizontal ladder or grid, appears to require substantially greater amounts of lateral and ventral white matter in addition to some sparing of axons in the dorsal columns (Schucht et al., 2002; McEwan and Springer, 2006).

In order to translate our understanding of the relationships between tissue sparing and functional recovery to the clinical arena, outcome measures and imaging modalities common to both the basic research laboratory and clinic need to be established. Currently, acute management of spinal cord injuries relies on the ASIA score as a primary functional prognostic tool and a combination of standard imaging techniques including x-ray, CT and MR (Ishida and Tominaga, 2002; Miyanji et al., 2007). CT and the current standard MR imaging is sufficient to provide a gross understanding of the spinal level(s) involved and the primary features of the injury (Van Goethem et al., 2005; Furlan et al., 2007; Lammertse et al., 2007) including classification as a burst fracture, sub-luxation injury, SCIWORA or other (Furlan et al., 2007), however, modalities that provide further insight into the functional capacity of spared tissue and the potential for functional improvement is currently lacking.

Diffusion Tensor Imaging (DTI) detects central nervous system (CNS) tissue structure through the anisotropic diffusion of water molecules, reflecting the directional organization of barriers to water movement, including cell membranes, cytoskeletal components and extracellular matrices (Le Bihan, et al., 2001; Basser and Jones, 2002; Yablonskiy, et al., 2003; Jones, et al., 2005; Le Bihan, 1995, 2006;). The structure of the normal spinal cord, with the gray matter compartment surrounded by fairly homogeneous white matter funiculi, is an ideal model for the application of DTI sequences designed to focus on distinguishing white matter from gray and, further, for distinguishing pathological and non-functional white matter from functional (Loy et al., 2007; Mogatadakala and Narayana, 2009; Sundberg et al., 2010). We showed recently, using a mouse model of SCI, that changes in axial diffusivity at 3 hours post-injury are predictive of gross locomotor function at 2 weeks as assessed by the Basso Mouse Scale (Basso et al., 2006; Kim et al., 2010).

In the current study a standard rat model of T9 contusive spinal cord injury was used to explore the relationship between the hyperacute diffusivity in the lateral and ventral white matter at the injury epicenter and the long-term recovery of hindlimb locomotor activity. *In vivo* diffusion tensor imaging of the injury epicenter was completed within 3 hours of injury while a comprehensive set of behavioral and electrophysiological outcome measures were used to assess hindlimb function at 4 weeks post-injury. Translating these approaches to the clinical situation will allow critical decisions to be made with a much stronger understanding of the future functional status of any anatomically contiguous spinal cord tissue leading to better outcomes.

Methods

Spinal cord injuries

Fourteen female Sprague-Dawley rats (225-250g) were used for this experiment. All procedures involving experimental animals were performed according to the guidelines of, and with the expressed permission of the Institutional Animal Care and Use Committees at Washington University in St. Louis and the University of Louisville. Each animal was anesthetized with ketamine/xyalzine (80mg/Kg & 10mg/Kg, ip) and given prophylactic antibiotics (gentamicin sulfate, 15mg/kg, sc). Three animals received sham injuries and the remaining eleven animals received contusion injuries of 1.00 (very mild; n=3), 1.25 (mild; n=3) or 1.5mm (moderate; n=4) displacement using a custom designed electromagnetic force driven impactor. The contusion injuries were delivered to the T9 spinal cord following a T8 laminectomy. Due to a technical error, one animal received an injury of approximately 1.75mm displacement. We have included data from this animal where appropriate, but not for the statistical analysis of group data due to its outlier status.

Acute Diffusion Tensor Imaging

One day prior to receiving an injury, three animals were randomly selected for DTI imaging. The DTI measures of these naïve rats were not statistically different from those of the sham controls that were imaged hyperacutely (at 3 hours, data not shown). Naïve and sham control DTI measures were thus combined to represent normal “uninjured” values for statistical analyses (n=6). The *in vivo* DTI setup and detailed procedures were similar to those reported previously (Kim et al., 2006). Briefly, following spinal cord injury, each rat was anesthetized with an isoflurane and oxygen mixture (0.2 – 1.5%) and underwent *in vivo* DTI examination (Kim, et al., 2006). A circulating warm water pad was used to maintain core body temperatures at 37°C. The respiratory exhaust line was connected to a pressure transducer where a TTL signal was generated to synchronize the DTI data acquisition to the animal's respiratory motion. A 12cm inner diameter Helmholtz coil was employed as the RF transmitter. An inductively-coupled surface coil covering the T8 – T10 vertebral segments (30mm × 20mm) was used as the receiver. The whole preparation was placed in an Oxford Instruments 200/330 magnet (4.7T, 33cm clear bore) equipped with a 15cm inner diameter, actively shielded Magnex gradient coil (18G/cm, 200-μs rise time). The Varian UNITY-INOVA console, controlled by a Sun Blade 1500 workstation (Sun Microsystems, Santa Clara, CA), was used to interface the magnet, gradient coils, and Techron gradient power supply. Due to respiratory gating, the repetition time (TR, ~ 2.2s) was slightly varied among animals with fixed echo time (TE) at 35ms. Images were obtained with diffusion sensitizing gradients applied in six orientations: (Gx,Gy,Gz) = (1,1,0), (1,0,1), (0,1,1), (-1,1,0), (0,-1,1), and (1,0,-1). Two diffusion-sensitizing b values, 0 and 1.0 ms/μm^2, were used with time between application of gradient pulses (Δ) = 18ms and diffusion gradient on time (δ) = 7ms. Two scans were averaged per k-space line with a field of view of 20mm × 20mm and a data matrix of 128 × 256 (zero filled to 256 × 256). Ten transverse images with a slice thickness of 1.5 mm were collected covering the vertebral segments T8 – T10 in 1.5 hours (30min for MR setup/planning and 1 hour for *in vivo* DTI).

Following the acute DTI, animals were handled daily and assessed weekly at Washington University using the BBB Scale. At 24 days post-injury the animals were transferred to the Kentucky Spinal Cord Injury Research Center at the University of Louisville for 3 days of intensive assessment.

In Vivo DTI Data Analyses

The *in vivo* DTI data were analyzed using custom software written in Matlab (MathWorks, Natick, MA, USA). Briefly, the diffusion tensors were derived independently for each voxel

from the diffusion-weighted images using a weighted linear least-squares method (Koay et al., 2006). For each tensor, the eigenvalue decomposition was then applied, yielding a set of eigenvalues ($\lambda_1 \geq \lambda_2 \geq \lambda_3$) and eigenvectors for each voxel. Maps of diffusion indices of the axial diffusivity ($\lambda\parallel$), radial diffusivity ($\lambda\perp$), relative anisotropy (RA), and mean diffusivity (<D>) were derived according to Eqs. [1] – [4]:

$$\lambda \parallel = \lambda_1 \quad [1]$$

$$\lambda \perp = (\lambda_2 + \lambda_3)/2 \quad [2]$$

$$<D> = (\lambda_1 + \lambda_2 + \lambda_3)/3 \quad [3]$$

$$RA = \frac{\sqrt{(\lambda_1 - <D>)^2 + (\lambda_2 - <D>)^2 + (\lambda_3 - <D>)^2}}{\sqrt{3}\ <D>} \quad [4]$$

Functional and Electrophysiological Assessments

Assessments were performed by the fully trained Core and Laboratory staff members of the Kentucky Spinal Cord Injury Research Center at the University of Louisville. All scorers/assessors were blinded to the injury groups. Animals were assessed using the BBB Open Field Locomotor Scale, digital gait analysis for stepping and the Louisville Swim Scale and kinematics for swimming (Basso et al., 1995; Smith et al., 2006b; Hamers et al., 2006; Magnuson et al., 2009). In addition, sensory-motor (precision stepping) was assessed using the horizontal ladder task (McEwan and Springer, 2006). Finally, transcranial magnetic motor-evoked potentials were used to assess action potential conduction across the injury site in the ventrolateral white matter (tcMMEPs; Magnuson et al., 1999) and the magnetic inter-enlargement response was used to assess conduction in the lateral white matter (MIER; Beaumont et al., 2006).

Each animal was assessed using the BBB 22-point (0-21) Open Field Locomotor Scale (Basso et al., 1995). The scoring was performed by 2 experts over a 4 minute period while the animals moved around in an open field (plastic wading pool, 36” in diameter). The BBB Scale is divided into three categories; the low end of the scale (0-7) assesses hindlimb movements in the absence of stepping or plantar paw placement, the middle part of the scale (8-13) evaluates weight support at stance, uncoordinated stepping and occasional to frequent coordination while the high end of the scale (14-21) uses weight support during stepping, consistent interlimb coordination and tail position. Digital gait analysis involved assessing foot placement order from ventral-view video taken while the animals walked down a plexiglass runway. We use a modification of the standard Regularity Index (RI) as developed by Hamers and Koopmans (Hamers et al., 2006). This modification involves calculating the ratio of the number of plantar hindlimb steps that occur in one of the 3 correct orders with respect to the forelimb paw placements (cruciate, alternate or rotary) over the total number of forelimb steps expressed as a decimal. Thus, if an animal achieves 4 correctly ordered hindimb steps out of a total of 10 complete step cycles, they will score 0.4 and will be considered to have poor FL-HL coordination. Hindimb steps that do not occur in a correct order are not counted. Animals that score between 0.5 and 1.0 are considered to have recovered occasional to consistent forelimb-hindlimb coordination.

The Louisville Swim Scale (LSS) is an 18-point scale (0-17) based loosely on the BBB, that grades how animals swim in 4-minute sessions swimming lengths in a 60” plexiglass pool

with an exit ramp at one end. Normal animals use their hindlimbs only for propulsion, use exclusively a right-left hindlimb alternation and maintain a horizontal body position. Post injury, animals rely on their forelimbs for forward motion and have difficulty maintaining a normal body position (angle and rotation). For the LSS, the animals are scored on their primary body position, forelimb dependence, hindlimb movement and hindlimb alternation (Smith et al., 2006). In addition to the LSS, swimming was assessed kinematically where stick figures are created from digital video and are used to calculate the change over time in the angles created by the iliac crest – hip – ankle (IHA) and hip – ankle – toe (HAT) segments for 6-9 representative stroke cycles at each time point. IHA vs HAT plots are analyzed to estimate the area (representing the out-of-phase angular excursions) and centroid (representing the median limb position). Finally, the toe velocity relative to the hip is calculated to provide an indication of the forces being generated during the swimming stroke. The pattern and effectiveness of the hindlimb movements can thus be described for each animal at each time point via the area and centroid of the angle-angle plot, plus the toe velocity (Magnuson et al., 2009).

The horizontal ladder assessments were performed by trained staff blinded to the injury groups, as described by Bolton and colleagues (2006). Animals were assessed using the Columbus Instruments horizontal ladder with automated counting where footfalls that make contact with a stainless steel plate located 3 cm below the ladder rungs are registered automatically. In addition, two observers counted footfalls manually. These counts were used to verify the automated system and in the case of operator error where the automated counter was re-set incorrectly. These assessments were done with minimal pre-exposure of the animals to the device, which provides the advantage of novelty and resulted in very consistent results. Each animal was assessed three times a day on two consecutive days. The error counts were averaged for all trials.

We performed the tcMMEP and MIER electrophysiological assessments in single procedures without anesthesia as described previously (Magnuson et al., 1999 and Beaumont et al., 2006). Briefly, animals are held firmly, ventral surface down with limbs extended, on a piece of white pine using push pins and a 6” × 8” cloth stockinette. Pairs of stainless steel needle electrodes (recording) are placed into the medial gastrocnemius (tcMMEP) or triceps (MIER) muscles and a single ground electrode is placed in the base of the tail (tcMMEP) or nape of the neck (MIER). Magnetic stimuli (70μs) are applied to the skull (tcMMEP) with a 50mm round transducer or to one hip (MIER) by a 25mm figure-8 transducer (MagStim 200). EMG responses are recorded at approximately 6ms latency. The amplitude of the responses for the tcMMEP are dependent on action potential conduction in descending axons within the medial aspect of the ventrolateral funiculus (Loy et al., 2002a, 2002b) and for the MIER, on ascending axons within the outer aspects of the lateral funiculus (Beaumont et al., 2006).

Statistical Analyses

Differences between the injury groups’ BBB, LSS, horizontal ladder and swimming kinematics at 4 weeks post-injury were analyzed with one-way analysis of variance, followed by Tukey HSD *post hoc* t-tests, when appropriate. Pearson or Spearman Rank correlation coefficients were calculated (as appropriate) to compare interrelationships between axial diffusivity, % spared white matter (at 28 days), % normal white matter (at 3 hours) and functional recovery. All analyses were performed using SPSS statistical package, v11.

Results

Diffusion Tensor Imaging

DTI scans were completed for all animals within 3 hours of injury. Scans were performed on the thoracic spinal cord including a region spanning one to two segments rostral and caudal to the T9 injury epicenter. Figure 1 shows the axial diffusivity ($\lambda\perp$), describing water diffusion along axonal fibers), radial diffusivity ($\lambda\perp$) describing water diffusion perpendicular to axonal fibers) and relative anisotropy (RA) maps of spinal cords from 1 sham (A) and 1 moderately injured (1.5mm severity) rat (B). The white matter tracts exhibited high axial diffusivity, approximately six times the radial diffusivity, reflecting axon microstructure as previously reported (Kim, et al., 2007a, Kim, et al., 2007b). The gray matter axial and radial diffusivity were comparable reflecting a characteristic isotropic diffusion. The anisotropic white matter and isotropic gray matter were clearly distinguishable in the RA maps. The contusion-induced white matter damage was observable as significant image intensity reductions in the axial diffusivity maps (B, top row). In contrast, radial diffusivity maps exhibited only minor image intensity reductions in the injured white matter (B, middle row). Acutely, the contusion-induced ventral and lateral white matter damage was most severe near the epicenter. Evidence of dorsal column and corticospinal tract damage is seen in both $\lambda\parallel$ and $\lambda\perp$ maps over the entire length of scanned spinal cord. Gray matter damage is visible in the dorsal horns extending caudally into the region of the central canal in the middle 3 MR image slices, which also contained the most severely damaged ventral and lateral white matter (Figure 1B).

In Figure 2 we compare the $\lambda\parallel$ maps at 3 hours post-injury that were manually segmented (red outlines) or segmented in an automated fashion using a $\lambda\parallel$ threshold (yellow outlines). The manual segmentation was performed visually using the gray/white matter contrast provided by $\lambda\parallel$ and RA (Figure 1A and B) that are not sensitive to injury, acutely (Kim et al., 2010). Consequently, manual segmentation produced maps of total ventral and lateral white matter, excluding the dorsal columns. The automated segmentation was performed using a $\lambda\parallel$ threshold limit (mean ± 2×SD) measured from the 6 sham and naïve rats, as described previously (Kim et al., 2010). Therefore, automated segmentation provided an estimate of cross-sectional area of white matter with near-normal $\lambda\parallel$ (yellow outlines, “normal appearing white matter” or NWM).

Behavioral Assessments

Following acute DTI scanning, animals were assessed at Washington University using the BBB Open Field Locomotor Scale at 1, 4, 7, 11, 14, 18, 21 and 24 days post-injury. With one exception, injured animals showed very little improvement from day 1 to day 4, but all showed dramatic increases in BBB score between days 4 and 14, and very little change thereafter (Figure 3). Eight animals that scored 4 or under on day 4 had scores that fell into three functionally distinct ranges on day 24; 3 showed weight supported stepping with coordination (BBB 14-16), 4 showed weight supported stepping without coordination (BBB 10-11) and one did not achieve plantar paw placement at any time point (BBB = 5). Three animals with very mild injuries that scored between 6.5 and 11 on day 1 were not distinguishable from sham animals at day 24. The animals were then assessed intensively over a three-day period at the University of Louisville as described below.

Swimming and Stepping Assessments

Figure 4 shows the results of the swimming (A-C) and stepping (D-F) assessments from post-injury days 25-27 plotted against the % NWM at 3 hours post-injury as shown in Figure 2. The LSS was not able to distinguish between the sham animals and those with very mild (1.00mm) injuries, but did find significant differences between the very mild, mild

(1.25mm) and moderately injured (1.5mm) groups ($p<.05$). In contrast, with the exception of the severely injured outlier, all the animals were able to achieve near-normal angle-angle plot areas (over 30 degrees squared; Figure 4B). These areas represent the angular excursions of the IHA (iliac crest-hip-ankle) and HAT (hip-ankle-toe) angles for each kick, and larger areas represent larger limb movements with good intra-limb coordination. The high sensitivity of this measure did show that the animals with moderate injuries had significantly lower ellipse areas than the shams and than animals with very mild injuries ($p<.05$; Figure 4B). The maximum toe velocity during the extension (propulsive) phase also distinguished between the moderately injured and very mildly injured groups suggesting that the animals with 1.5mm injuries were unable to generate normal extensor (propulsive) forces when kicking ($p<.05$; Figure 4C).

The BBB and horizontal ladder task showed that the mild and moderately injured animals were significantly different from the uninjured and sham groups, and from each other ($p<.05$; Figure 4D & F). Gait assessment revealed significant variability in the Regularity Index, a measure of paw placement order. Interestingly, one of the animals with mild injuries and all three animals with very mild injuries recovered near-normal paw placement order ($RI > 0.6$) while two of the animals with moderate injuries and all of the animals in the moderate group did not ($RI \leq 0.4$). The single outlier, with very significant functional deficits ($BBB < 8$), was not able to achieve plantar stepping and thus was not included in the Regularity Index or Horizontal Ladder assessments. None of the stepping assessments were able to distinguish between the sham and very mild groups. Unexpectedly, the horizontal ladder revealed a fairly linear increase in foot placement errors with increasing severity.

Importantly, all these locomotor assessments (Figure 4, A-F) are significantly correlated to % NWM determined at 3 hours post-injury using automated segmentation of $\lambda\|$ as shown in Figure 2. Table 1 shows that these correlations range from 0.83 (r^2) for the BBB scores to 0.47 for the angle-angle plot areas, when the sham group is not included.

Electrophysiological Assessments & Diffusion Tensor Imaging

At 4 weeks post-injury the experimental animals could be divided into 4 different groups based on their tcMMEP and MIER responses (Figure 5). As shown previously (Loy et al., 2002a; 2002b), the tcMMEP response is carried in the ventrolateral funiculus and is exquisitely sensitive to contusion injuries. In contrast, the MIER is carried in the lateral funiculus, is less sensitive to contusion injury and correlates well with overground stepping (Beaumont et al., 2006). Only sham animals had intact tcMMEPs, while the 3 animals with very mild injuries, and one animal with a mild injury had intact MIER responses. The other two animals with mild injuries had MIER responses with delayed latencies, and the four animals with moderate injuries lacked both tcMMEP and MIERs. Based on these electrophysiological profiles, each animal was assigned an electrophysiological score (from 1 to 4) as shown in Figure 5A. The regions of white matter known to carry the descending tcMMEP and ascending MIER responses at the thoracic site of injury were used to delineate regions of interest (ROIs) respectively in the ventrolateral and lateral funiculi at the level of the central canal as shown in Figure 5B. These ROIs were subsequently divided into inner and outer regions in an effort to reflect their respective sensitivities to being disrupted by contusion injuries.

DTI derived $\lambda\|$ within the ROIs of the inner and outer ventrolateral and outer lateral funiculi ranged from 0.75 to 2.25 at 3 hours post-injury, with decreased $\lambda\|$ reflecting axonal injury. Figure 6 shows the $\lambda\|$ at 3 hours for the inner ventrolateral (VLF) and outer lateral funiculi (LF) plotted against the tcMMEP and MIER amplitudes (A & C) and latencies (B & D) at 4 weeks. These regions of interest showed increases in action potential conduction at 4 weeks post-injury, reflected as increases in hindlimb EMG response amplitudes or normal (shorter)

response latencies when axial diffusivity measured at 3 hours post-injury was approximately 1.5μm^2/ms or above.

Terminal Histology and % NWM Determined by DTI

In Figure 7A we show representative images of EC (eriochrome cyanin) stained sections from the injury epicenters of the four primary experimental groups. Percent spared white matter (SWM), determined histologically at 4 weeks, is plotted against % NWM predicted by automated segmentation of DTI derived $\lambda\|$ maps at 3 hours. The predicted NWM and actual SWM are strongly correlated with or without inclusion of the sham group (r^2=.95 or . 88, respectively; Figure 7B).

Discussion

This experiment involved two sites, Washington University in St. Louis, where the animals were injured, imaged and assessed using the BBB Open Field Locomotor Scale, and the University of Louisville, where the animals were intensively assessed over a 3 day period using a battery of behavioral, electrophysiological and histological measures. We showed previously that hyper-acute DTI was predictive of long-term overground locomotor function and ventral and lateral white matter integrity in a mouse model of SCI (Kim et al., 2010). The current study was undertaken to move this concept into a rat model thus permitting the use of *in vivo* electrophysiology in addition to a more comprehensive set of objective locomotor assessments. Thus, our goal was to thoroughly assess the potential role of hyper-acute diffusion tensor imaging as a prognostic tool, or functional biomarker, for spinal cord white matter after contusive injuries.

Behavioral Outcomes

At 1 and 4 days post-injury, the BBB scores divided grossly into three groups; animals that displayed very little hindlimb movement (<5, n=8), animals that had moderate to extensive movement, some with plantar placement and stepping (BBB 7-17, n=3) and a group that were normal, scoring 20 or 21 (n=3; Figure 3). The first group had received mild (1.25mm; n=3) or moderate (1.5mm, n=4) injuries and included the outlier that received a severe injury. As anticipated, the BBB scores reached a plateau by day 14, and by day 24 these 8 animals fell into two groups with the mildly injured animals reaching a BBB score of 14-16, the moderately injured animals scoring 10-11 and the outlier scoring a 5. With the exception of the very mildly injured animals, the BBB scores at 1 and 4 days post-injury were not predictive of the scores recorded at day 24. This is likely due to spinal shock, where the normal activity of spinal cord neurons is disrupted, even far caudal to the injury site, resulting in flaccid paralysis and minimal hindlimb movement acutely (Ditunno et al, 2004). These observations are in keeping with those published previously by many laboratories, and in particular are grossly similar to the findings of Basso et al. (2002) who used mild and moderate contusion injuries at T9. Using daily BBB assessments, they found that both groups scored 5 or less on days 1 and 2, but separated out to mean scores of 17 and 12 by day 28 post-injury. Importantly, gait assessment revealed that all the mildly injured rats recovered forelimb-hindlimb coordination while the moderately injured animals did not.

Assessment of the animals at the University of Louisville involved both stepping and swimming, a combination that allows hindlimb movement to be evaluated with and without the concomitant requirement for weight support (Figure 4). Swimming was evaluated using the Louisville Swim Scale and kinematically (Smith et al., 2006b; Kuerzi et al., 2010). We employed angle-angle plots to described the overall hindlimb excursion and intralimb coordination and the toe velocity (relative to the hip) to describe the extensor forces generated during the propulsive phase of the swimming stroke. With the exception of the

severely injured outlier, all the animals were able to generate strokes with substantial angle-angle plot areas, however, the animals with moderate injuries (1.5mm) were unable to generate toe velocities greater than 60mm/s, approximately half that of normal or very mildly injured animals. A kicking pattern that lacks propulsive force is not able to propel the animals leading to poor overall swimming ability and LSS scores less than 8. None of the swimming assessments could distinguish between the sham and very mild group suggesting that there is a threshold of white matter sparing above which deficits in swimming are not easily detected. Overall, these findings suggest that, in the absence of a requirement for weight support, a quality swimming pattern can be generated by animals with a wide range of injury severities, however, normal propulsive forces and body posture during kicking requires greater amounts of white matter sparing at the epicenter and were achieved only by the mildly and very mildly injured groups. These findings mimic our previous observations for animals that did not receive additional swim training as a rehabilitation strategy (Smith et al., 2006b).

Stepping was evaluated using the BBB Scale, a gait assessment (the Regularity Index) and the horizontal ladder task. Animals with moderate injuries made a substantial number of errors on the horizontal ladder, had RIs less than 0.5 indicating a lack of forelimb hindlimb coordination, and did not score above a 12 on the BBB scale. Hindpaw placement was not related to the placement of the homolateral forepaw, and the forelimbs and hindlimbs appeared be controlled independently. Animals with mild injuries had RIs indicating that one regularly achieved correct paw placement (RI > 0.6) while two did not. This functional difference resulted in BBB scores that straddled the cut-off of 14 indicating the presence/absence of forelimbhindlimb coordination. These data suggest a significant behavioral break point at the mild injury severity for forelimb-hindimb coordination (BBB = 13-15; RI = 0.4-0.6). It is very interesting to note that both of the behavioral scales employed, the BBB and the LSS, were able to distinguish between the very mild and mild groups, whereas these groups were not distinguishable using swimming kinematics, toe velocity, the RI or the horizontal ladder task.

Diffusion Tensor Imaging

We used the contrast provided by the $\lambda\perp$ and RA maps to manually segment the spinal cord white matter in images taken from hyper-acute (3 hours post-injury) DTI scans. In these same images, we utilized automated segmentation, based on the $\lambda\parallel$ (mean ± 2 × SD) derived from scans of 6 uninjured or sham animals, to outline the normal appearing white matter in all the animals at 3 hours post-injury (Figure 2). These images show the expected narrow rim or rind of normal appearing white matter in animals with very mild or mild injuries, and broken islands or patches of white matter with near-normal axial diffusivity around the edges in moderately injured spinal cords. These segmented images were then used to calculate the % normal appearing white matter at 3 hours, which was found to strongly correlate with both functional outcomes at 4 weeks post-injury (Figure 4, Table 1), and with the % spared white matter determined histologically (Figure 7). The strength of these correlations indicate that hyper-acute axial diffusivity of spinal cord white matter can be used to accurately predict long-term functional outcomes and long-term sparing of spinal cord white matter following clinically relevant contusive spinal cord injuries (Kim et a., 2010).

WM Regions of Interest for tcMMEPs and MIERs

We showed previously that tcMMEP and MIER responses are carried in the ventrolateral and lateral funiculi at T9, respectively, and that both these responses are very sensitive to injury (Loy et al., 2002; Beaumont et al., 2006). Based on our previous work utilizing lesions that either spared or abolished the tcMMEP and MIER responses, we established

regions of interest (ROIs) in the medial VLF and lateral LF, respectively within which axial diffusivity was measured at 3 hours post-injury (Figure 5). Sham animals, with intact MMEPs, had λ∥ of 1.5μm^2/ms or greater at 3 hours in the medial VLF ROI, whereas all the lesioned animals had both a lack of a tcMMEP response and had ROI λ∥ below 1.5μm^2/ms within the medial VLF ROI. Among the injured animals, the group with very mild injuries and one animal with a mild injury had both intact MIERs and had a lateral LF ROI λ∥ that exceeded 1.5μm^2/ms. Similarly, all of the animals that lacked MIER responses of normal latency also had lateral LF λ∥ less than 1.5μm^2/ms at 3 hours post-injury (Figure 6). While further validation is required, these observations suggest that λ∥ of 1.5μm^2/ms at 3 hours post-injury represents a functional break point and that at least some of the axons in these regions of interest, known to carry the tcMMEP and MIER responses, had regained the capacity to conduct action potentials across the site of injury at 4 weeks. Automated segmentation based on uninjured white matter (Figure 2, bottom row) identified lateral and ventrolateral white matter that appeared normal (or spared) at 3 hours post-injury that overlapped with the ROIs for tcMMEP and MIER responses. Thus, we speculate that DTI-derived λ∥ can be used acutely, during the period of spinal shock, to specifically identify tracts and regions of white matter that will recover the capacity to conduct action potentials, and more generally to determine an estimate of white matter sparing. It is very interesting to note that the one mildly injured animal that retained an MIER with normal latency had an RI of almost 0.8 (good forelimb-hindlimb coordination, as discussed earlier), while the other two animals with mild injuries had delayed MIER responses and achieved an RI of only 0.4, indicating that they had poor forelimb-hindlimb coordination.

Conclusions

These results demonstrate, first of all, that acute locomotor scores are poor predictors of future functional status after a contusive spinal cord injury. Secondly, that DTI-derived λ∥ can be used hyper-acutely to accurately assess the percentage of normal appearing white matter, post-injury, and that this percentage correlates strongly with both functional outcomes and terminal histological measures of spared white matter. Finally, hyperacute DTI can be used to predict the future functional status of white matter, as confirmed by *in vivo* electrophysiological measures; white matter regions with λ∥ greater than 1.5μm^2/ms at 3 hours post-injury appear to contain at least some axons that are electrophysiologically intact and able to conduct action potentials at 4 weeks post-injury. Thus, in the clinical setting, DTI-derived λ∥ measures could be used acutely to provide an accurate prognosis of long-term white matter function and integrity, thus reducing the current reliance on functional outcomes in the form of the ASIA scale, reflex measures or other functional clinical examinations that should not be expected to have great prognostic value when used acutely.

Acknowledgments

The authors wish to thank the outstanding core personnel at KSCIRC; Kim Fentress, Christine Yarberry and Johnny Morehouse. Excellent technical assistance was provided by Alice Shum-Siu, Ashley Whelan and Edward Brown. This work was supported by a grant from the Kentucky Spinal Cord and Head Injury Research Trust to DSKM and also by the NIH/NINDS (R01 NS052292 & R01 NS047592) and COBRE (P20 RR15576).

References

Basser PJ, Jones DK. Diffusion-tensor MRI: theory, experimental design and data analysis - a technical review. NMR Biomed. 2002; 15:456–67. [PubMed: 12489095]

Basso DM, Beattie MS, Bresnahan JC. A sensitive and reliable locomotor rating scale for open field testing in rats. J. Neurotrauma. 1995; 12:1–21. [PubMed: 7783230]

Basso DM, Beattie MS, Bresnahan JC. Graded histological and locomotor outcomes after spinal cord contusion using the NYU weight-drop device versus transection. Exp. Neurol. 1996; 139:244–56. [PubMed: 8654527]

Basso DM, Beattie MS, Bresnahan JC. Descending systems contributing to locomotor recovery after mild or moderate spinal cord injury in rats: experimental evidence and a review of literature. Restor. Neurol. Neurosci. 2002; 20:189–218. [PubMed: 12515895]

Basso DM, Fisher LC, Anderson AJ, Jakeman LB, McTigue DM, Popovich PG. Basso Mouse Scale for locomotion detects differences in recovery after spinal cord injury in five common mouse strains. J. Neurotrauma. 2006; 23:635–59. [PubMed: 16689667]

Beaumont E, Onifer SM, Reed WR, Magnuson DS. Magnetically evoked inter-enlargement response: an assessment of ascending propriospinal fibers following spinal cord injury. Exp. Neurol. 2006; 201:428–40. [PubMed: 16797539]

Bolton DA, Tse AD, Ballermann M, Misiaszek JE, Fouad K. Task specific adaptations in rat locomotion: runway versus horizontal ladder. Behav. Brain Res. 2006; 168:272–279. [PubMed: 16406145]

Detloff MR, Clark LM, Hutchinson KJ, Kloos AD, Fisher LC, Basso DM. Validity of acute and chronic tactile sensory testing after spinal cord injury in rats. Exp. Neurol. 2010; 225:366–76. [PubMed: 20643128]

Ditunno JF, Little JW, Tessler A, Burns AS. Spinal shock revisited: a four-phase model. Spinal Cord. 2004; 42:383–95. [PubMed: 15037862]

Fehlings MG, Furlan JC, Massicotte EM, Arnold P, Aarabi B, Harrop J, Anderson DG, Bono CM, Dvorak M, Fisher C, France J, Hedlund R, Madrazo I, Nockels R, Rampersaud R, Rechtine G, Vaccaro AR. Interobserver and intraobserver reliability of maximum canal compromise and spinal cord compression for evaluation of acute traumatic cervical spinal cord injury. Spine (Phila Pa 1976). 2006; 31:1719–1725. [PubMed: 16816769]

Furlan JC, Fehlings MG, Massicotte EM, Aarabi B, Vaccaro AR, Bono CM, Madrazo I, Villanueva C, Grauer JN, Mikulis D. A quantitative and reproducible method to assess cord compression and canal stenosis after cervical spine trauma: a study of interrater and intrarater reliability. Spine (Phila Pa 1976). 2007; 32:2083–2091. [PubMed: 17762809]

Gale K, Kerasidis H, Wrathall JR. Spinal cord contusion in the rat: behavioral analysis of functional neurologic impairment. Exp. Neurol. 1985; 88:123–34. [PubMed: 3979506]

Hamers FP, Koopmans GC, Joosten EA. CatWalk-assisted gait analysis in the assessment of spinal cord injury. J. Neurotrauma. 2006; 23:537–48. [PubMed: 16629635]

Hiersemenzel LP, Curt A, Dietz V. From spinal shock to spasticity: neuronal adaptations to a spinal cord injury. Neurology. 2000; 54:1574–82. [PubMed: 10762496]

Ishida Y, Tominaga T. Predictors of neurologic recovery in acute central cervical cord injury with only upper extremity impairment. Spine (Phila Pa 1976). 2002; 27:1652–8. discussion 1658. [PubMed: 12163727]

Jones DK, Symms MR, Cercignani M, Howard RJ. The effect of filter size on VBM analyses of DT-MRI data. Neuroimage. 2005; 26:546–554. [PubMed: 15907311]

Kim JH, Budde MD, Liang HF, Klein RS, Russell JH, Cross AH, Song SK. Detecting axon damage in spinal cord from a mouse model of multiple sclerosis. Neurobiol. Dis. 2006; 21:626–632. [PubMed: 16298135]

Kim JH, Loy DN, Liang HF, Trinkaus K, Schmidt RE, Song SK. Noninvasive diffusion tensor imaging of evolving white matter pathology in a mouse model of acute spinal cord injury. Magn. Reson. Med. 2007a; 58:253–260. [PubMed: 17654597]

Kim JH, Trinkaus K, Ozcan A, Budde MD, Song SK. Postmortem delay does not change regional diffusion anisotropy characteristics in mouse spinal cord white matter. NMR Biomed. 2007b; 20:352–359. [PubMed: 17451177]

Kim JH, Loy DN, Wang Q, Budde MD, Schmidt RE, Trinkaus K, Song SK. Diffusion tensor imaging at 3 hours after traumatic spinal cord injury predicts long-term locomotor recovery. J. Neurotrauma. 2010; 27:587–98. [PubMed: 20001686]

Koay CG, Carew JD, Alexander AL, Basser PJ, Meyerand ME. Investigation of anomalous estimates of tensor-derived quantities in diffusion tensor imaging. Magn. Reson. Med. 2006; 55:930–6. [PubMed: 16526013]

Kuerzi J, Brown EH, Shum-Siu A, Siu A, Burke D, Morehouse J, Smith RR, Magnuson DS. Task-specificity vs. ceiling effect: step-training in shallow water after spinal cord injury. Exp. Neurol. 2010; 224:178–87. [PubMed: 20302862]

Kwo S, Young W, Decrescito V. Spinal cord sodium, potassium, calcium, and water concentration changes in rats after graded contusion injury. J Neurotrauma. 1989; 6:13–24. [PubMed: 2754736]

Lammertse D, Dungan D, Dreisbach J, Falci S, Flanders A, Marino R, Schwartz E. Neuroimaging in traumatic spinal cord injury: an evidence-based review for clinical practice and research. J. Spinal. Cord. Med. 2007; 30:205–214. [PubMed: 17684886]

Le Bihan D. Molecular diffusion, tissue microdynamics and microstructure. NMR Biomed. 1995; 8:375–386. [PubMed: 8739274]

Le Bihan D, Mangin JF, Poupon C, Clark CA, Pappata S, Molko N, Chabriat H. Diffusion tensor imaging: concepts and applications. J. Magn. Reson. Imaging. 2001; 13:534–546. [PubMed: 11276097]

Le Bihan D. [From Brownian motion to mind imaging: diffusion MRI]. Bull. Acad. Natl. Med. 2006; 190:1605–1627. discussion 1627. [PubMed: 17650747]

Leypold BG, Flanders AE, Burns AS. The early evolution of spinal cord lesions on MR imaging following traumatic spinal cord injury. Am. J. Neuroradiol. 2008; 29:1012–1016. [PubMed: 18296550]

Loy DN, Magnuson DS, Zhang YP, Onifer SM, Mills MD, Cao QL, Darnall JB, Fajardo LC, Burke DA, Whittemore SR. Functional redundancy of ventral spinal locomotor pathways. J. Neurosci. 2002a; 22:315–23. [PubMed: 11756515]

Loy DN, Talbott JF, Onifer SM, Mill MD, Burke DA, Dennison JB, Fajardo LC, Magnuson DS, Whittemore SR. Both dorsal and ventral spinal cord pathways contribute to overground locomotion in the adult rat. Exp. Neurol. 2002b; 177:575–80. [PubMed: 12429203]

Loy DN, Kim JH, Xie M, Schmidt RE, Trinkaus K, Song SK. Diffusion tensor imaging predicts hyperacute spinal cord injury severity. J. Neurotrauma. 2007; 24:979–990. [PubMed: 17600514]

McEwen ML, Springer JE. Quantification of locomotor recovery following spinal cord contusion in adult rats. J. Neurotrauma. 2006; 23:1632–53. [PubMed: 17115910]

Magnuson DS, Trinder TC, Zhang YP, Burke D, Morassutti DJ, Shields CB. Comparing deficits following excitotoxic and contusion injuries in the thoracic and lumbar spinal cord of the adult rat. Exp Neurol. 1999; 156:191–204. [PubMed: 10192790]

Magnuson DS, Lovett R, Coffee C, Gray R, Han Y, Zhang YP, Burke DA. Functional consequences of lumbar spinal cord contusion injuries in the adult rat. J. Neurotrauma. 2005; 22:529–43. [PubMed: 15892599]

Magnuson DS, Smith RR, Brown EH, Enzmann G, Angeli C, Quesada PM, Burke D. Swimming as a model of task-specific locomotor retraining after spinal cord injury in the rat. Neurorehabil. Neural. Repair. 2009; 23:535–45. [PubMed: 19270266]

Miyanji F, Furlan JC, Aarabi B, Arnold PM, Fehlings MG. Acute cervical traumatic spinal cord injury: MR imaging findings correlated with neurologic outcome--prospective study with 100 consecutive patients. Radiology. 2007; 243:820–7. [PubMed: 17431129]

Mogatadakala KV, Narayana PA. In vivo diffusion tensor imaging of thoracic and cervical spinal cord at 7 T. Magn. Res. Imaging. 2009; 27:1236–1241.

Schucht P, Raineteau O, Schwab ME, Fouad K. Anatomical correlates of locomotor recovery following dorsal and ventral lesions of the rat spinal cord. Exp. Neurol. 2002; 176:143–53. [PubMed: 12093091]

Schucht P, Raineteau O, Schwab ME, Fouad K. Anatomical correlates of locomotor recovery following dorsal and ventral lesions of the rat spinal cord. Exp. Neurol. 2002; 176:143–153. [PubMed: 12093091]

Smith RR, Burke DA, Baldini AD, Shum-Siu A, Baltzley R, Bunger M, Magnuson DS. The Louisville Swim Scale: a novel assessment of hindlimb function following spinal cord injury in adult rats. J. Neurotrauma. 2006a; 23:1654–70. [PubMed: 17115911]

Smith RR, Shum-Siu A, Baltzley R, Bunger M, Baldini A, Burke DA, Magnuson DS. Effects of swimming on functional recovery after incomplete spinal cord injury in rats. J. Neurotrauma. 2006b; 23:908–19. [PubMed: 16774475]

Sundberg LM, Herrera JJ, Narayana PA. In vivo longitudinal MRI and behavioral studies in experimental spinal cord injury. J. Neurotrauma. 2010; 27:1753–67. [PubMed: 20649481]

Van Goethem JW, Maes M, Ozsarlak O, van den Hauwe L, Parizel PM. Imaging in spinal trauma. Eur. Radiol. 2005; 15:582–90. [PubMed: 15696292]

Yablonskiy DA, Bretthorst GL, Ackerman JJ. Statistical model for diffusion attenuated MR signal. Magn. Reson. Med. 2003; 50:664–669. [PubMed: 14523949]

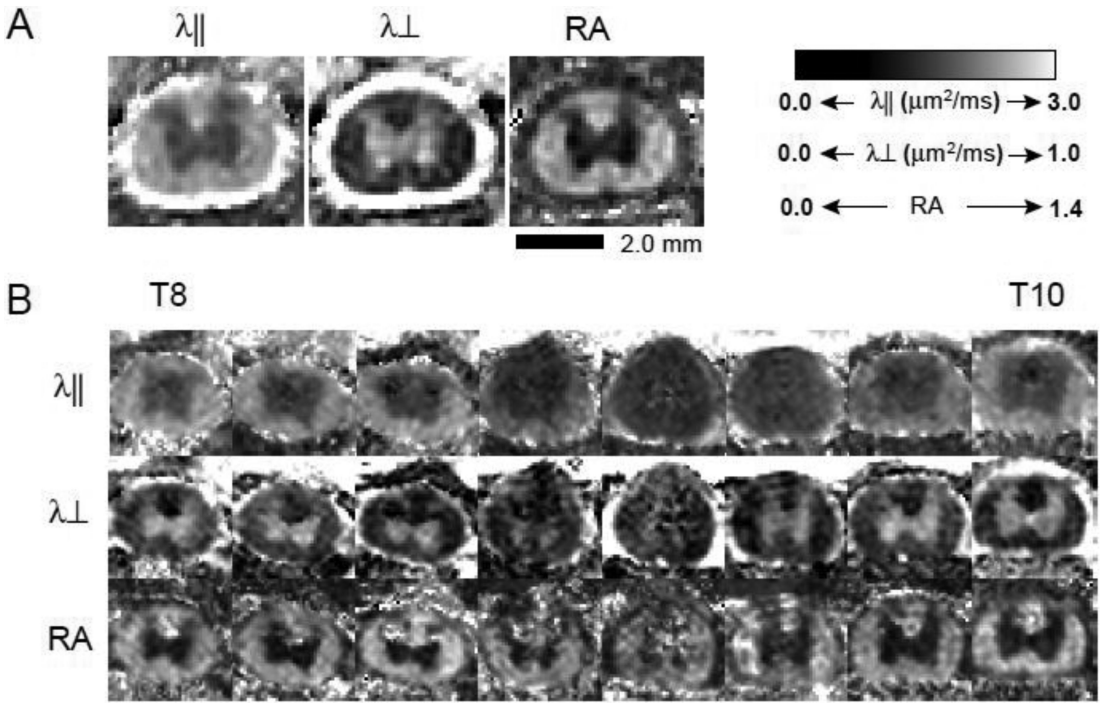

Figure 1.

A. Shown are representative acute *in vivo* diffusion tensor imaging (DTI) maps of a sham animal. Panels show axial diffusivity (λǁ), radial diffusivity (λ∞) and relative anisotropy (RA) maps. B. Panels show λǁ, λ∞ and RA DTI maps from T8 through T10 from one animal with a moderate (1.5mm) injury.

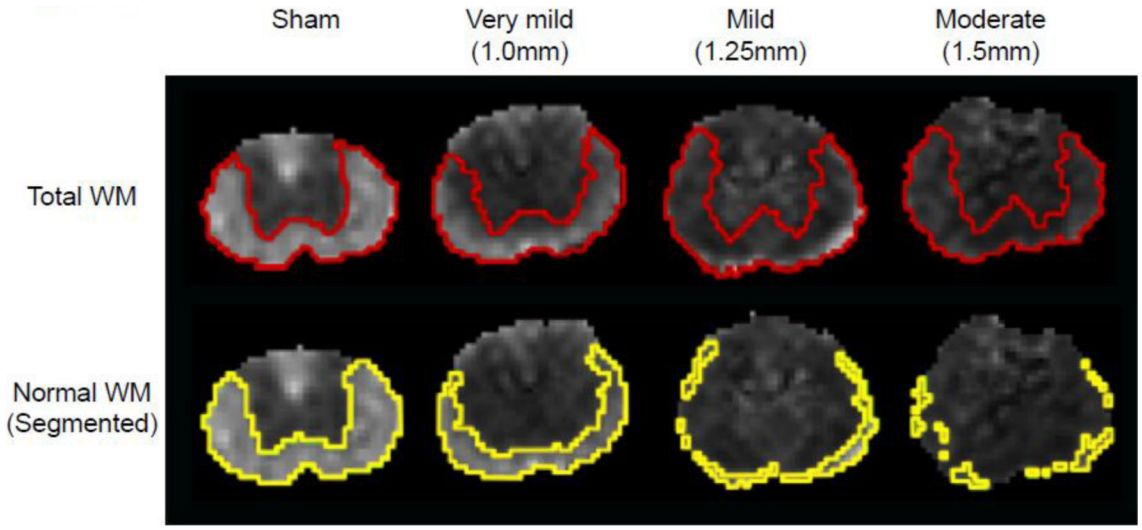

Figure 2.

Shown are acute axial diffusivity (λ∥) maps representative of the different injury severities examined. The red lines in the top panel indicate the white and gray matter delineation based on manual segmentation using the λ∥ and RA maps. The yellow line in the bottom panel represents the automated segmentation of normal white matter using the λ∥ of white matter (mean ± 2 × SD) as measured from the 6 naïve and sham control rats. This segmentation was used to calculate the % normal white matter (NWM) at 3 hours used in Figure 4 and Table 1.

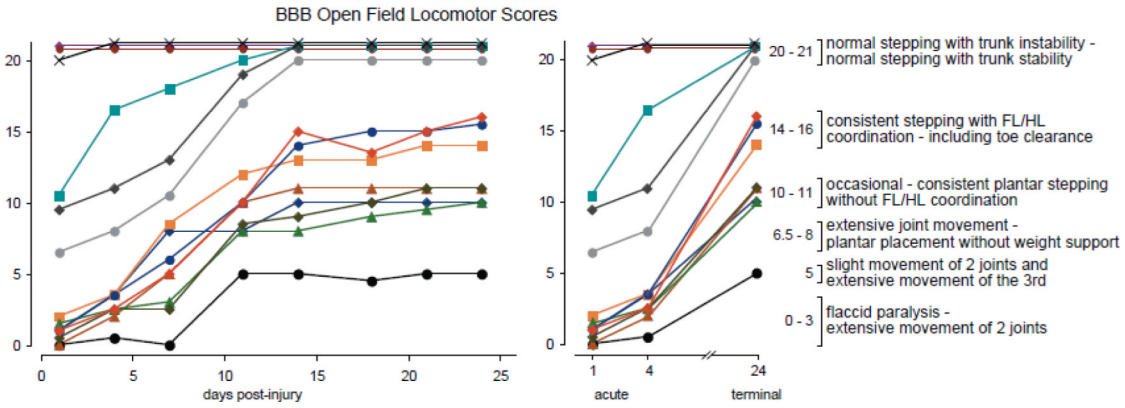

Figure 3.

BBB Open Field Locomotor Scores are shown for all the animals included in the study. Improvements in BBB Score were observed up to day 14 post-injury. The graph on the right shows the acute (days 1 & 4) and day 24 scores side-by-side for comparison. Animals with acute scores of 0-5 (days 1 & 4) had scores ranging from 5-16 at day 24.

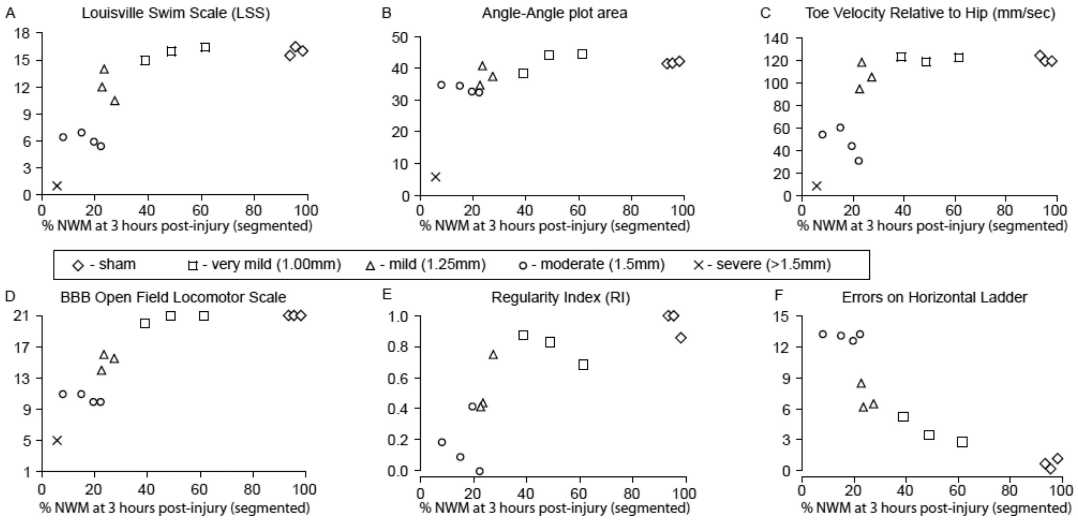

Figure 4.

Shown are terminal locomotor and sensorimotor scores for swimming (A-C) and overground stepping (D-F) at 27 days post-injury plotted against the % normal white matter determined using automated segmentation of the λǁ maps at 3 hours post-injury. The Louisville Swim Scale (A) and the BBB Open Field Locomotor Scale (D) are supplemented by objective kinematic (B & C), gait (E) and precision stepping (F) assessments. Correlations are shown in Table 1.

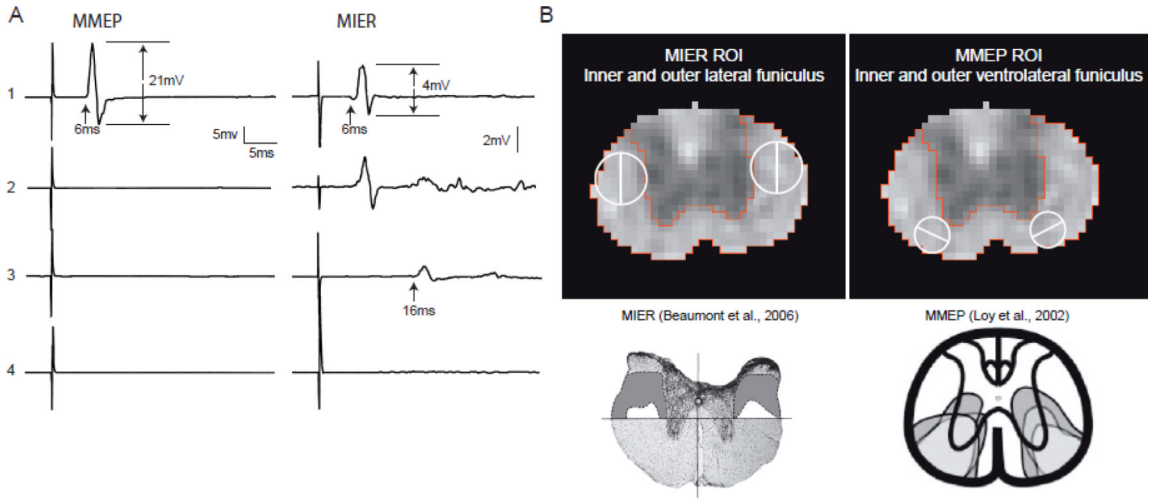

Figure 5.

A. Shown are representative tcMMEP and MIER EMG responses recorded from the gastrocnemius and triceps muscles, respectively, of animals with sham (1), very mild (2, 1.00mm displacement), mild (3, 1.25mm displacement) and moderate (4, 1.5mm displacement) contusion injuries. The analysis of the EMG responses included peak-to-peak amplitude in mV and latency in ms. B. Based on our previous work (Beaumont et al., 2006; Loy et al., 2002), we identified regions of interest (ROIs) in the lateral funiculus (LF) and ventrolateral funiculus (VLF) corresponding to the white matter tracks that carry the MIER and MMEP, respectively. These ROIs were then subdivided into inner (medial) and outer (lateral) halves based on the histologically determined pattern of white matter sparing following mild and moderate thoracic contusion SCIs.

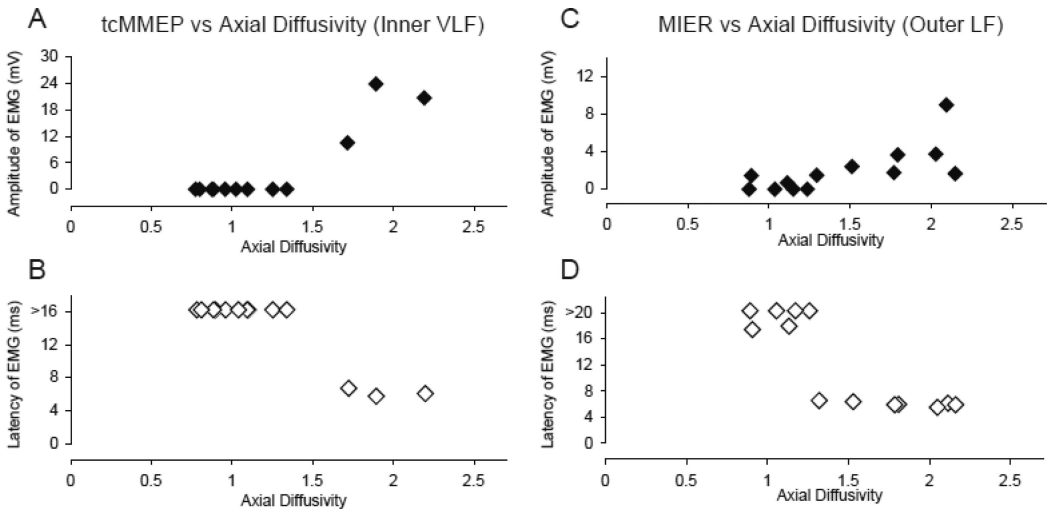

Figure 6.

Shown are plots of λ‖ of the inner VLF (A and B) and outer LF (C and D) ROIs vs the tcMMEP and MIER latency (A and C, respectively) and amplitude (B and D, respectively). Note that >16 in B and >20 in D represents no response within the time window analyzed (40ms). The tcMMEP and MIER response latencies are normal (~ 5ms) only if the inner VLF and outer LF ROIs show an λ‖ higher than 1.5 and 1.3μm^2/ms, respectively. The amplitudes of the tcMMEP and MIER responses increase when the respective ROIs exceed an λ‖ of 1.3-1.5μm^2/ms.

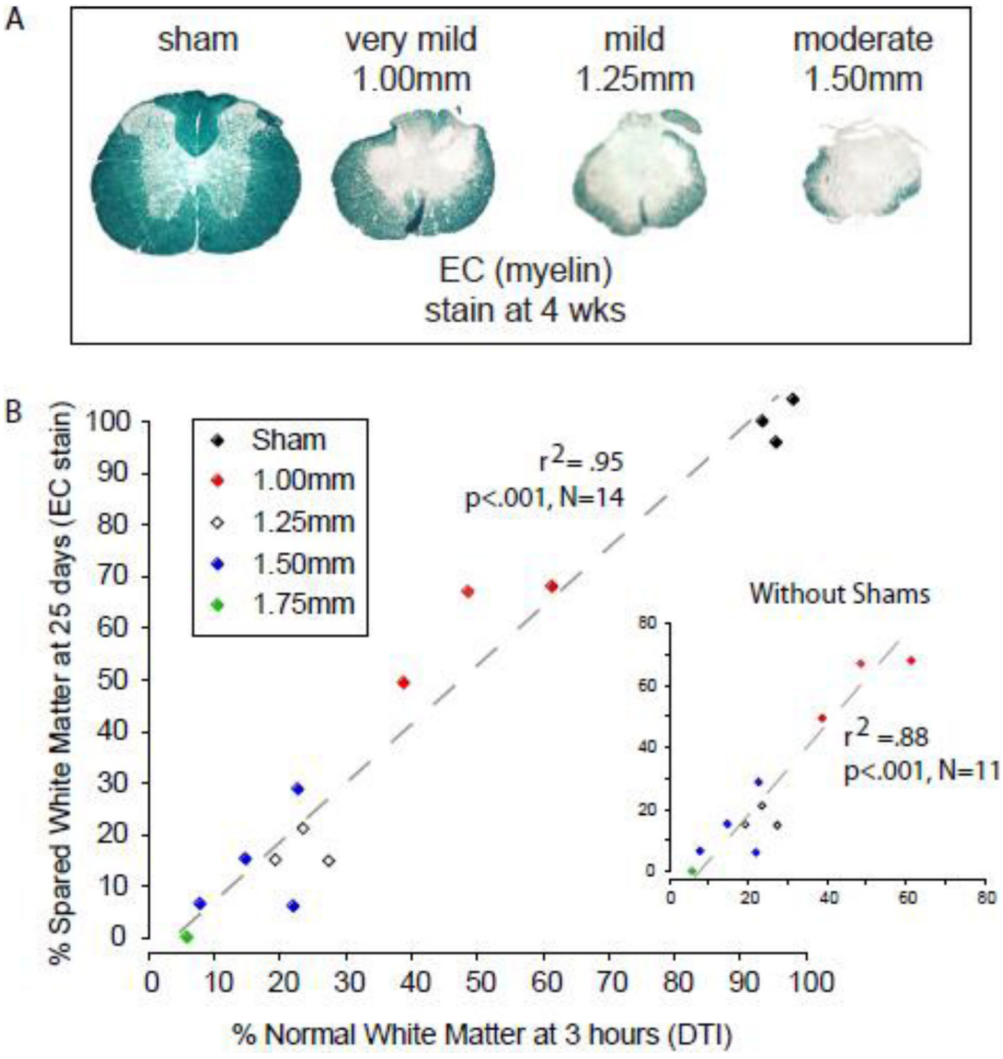

Figure 7.

A. Representative eriochrome cyanin (EC) stained histological sections of injury epicenters are shown for sham and each of the 3 injury severities. B. A scatter plot shows the relationship between the percent of normal white matter determined using automated segmentation from hyperacute (3 hour) DTI derived λ‖ and the percent spared white matter using end point histology (EC), with and without (inset) the group of sham animals.

Table 1

Correlations Between % Normal White Matter at 3h (DTI) and Function at 4 weeks

	all animals			no shams		
Assessment	**r**	**p**	**r^2**	**r**	**p**	**r^2**
LSS	.91	<.001	.82	.89	<.001	.79
A-A plot	.57	<.05	.33	.68	<.05	.47
toe vel	.69	<.01	.48	.77	<.01	.59
BBB	.94	<.001	.87	.91	<.001	.83
RI	.80	=.001	.64	.73	<.05	.53
ladder	-.89	<.001	.79	-.87	=.001	.75